



Pyrazole bridged binuclear transition metal complexes: Synthesis, characterization, antimicrobial activity and DNA binding/cleavage studies

Naveen V. Kulkarni, Anupama Kamath, Srinivasa Budagumpi, Vidyand K. Revankar *

Department of Chemistry, Karnatak University, Pavate Nagar, Dharwad 580 003, Karnataka, India

ARTICLE INFO

Article history:

Received 24 June 2011

Received in revised form 7 October 2011

Accepted 7 October 2011

Available online 14 October 2011

Keywords:

Pyrazole

Thiosemicarbazide

Antimicrobial activity

DNA binding study

Intercalation

ABSTRACT

A new ligand system having pyrazolato endogenous bridging component and N_4S_2 donating sites is synthesized by the condensation of 3,5-dichloroformyl-1H-pyrazole with phenylthiosemicarbazide. Both ligand and its binuclear Co^{II} , Ni^{II} , Cu^{II} and Zn^{II} complexes are characterized by the spectral and analytical methods. All the complexes were found to be binuclear monomeric in nature with octahedral geometry and nonelectrolytes. Electrochemical activity is observed only for the Cu^{II} complex in the applied potential range. Ligand and complexes were screened for antimicrobial activity and made to interact with *Escherichia coli* DNA to investigate the binding/cleaving ability by absorption, hydrodynamic, thermal denaturation and electrophoresis studies. The copper complex exhibited higher inhibition against a gram negative bacterium, *E. coli* and shown good intercalating ability with *E. coli* DNA.

© 2011 Elsevier B.V. All rights reserved.

1. Introduction

Pyrazole derivatives are the subject of many research studies due to their widespread potential biological activities such as anti-tumour [1], anti-inflammatory [2], antipyretic [3], antiviral [4], antimicrobial [1], anticonvulsant [5], antihistaminic [6], antidepressant [7], insecticides [8] and fungicides [8]. Pyrazoles are also used as antioxidant additives to fuels [9]. Pyrazole is very fascinating and significant to the coordination chemists, due to its 1,2-diazine unit which can provide the endogenous bridging between two similar or dissimilar transition or inner transition metal ions [10,11]. The appropriate ring substitutions especially at the 3 and 5 positions are expected to supplement the nucleophilicity and steric accessibility of the pyrazole nitrogens [10,12]. With the aid of other ligating functionalities incorporated through the ring substitution, the pyrazole derivatives can act as polydentate chelates and form stable coordination compounds of transition metal ions with greater specificity.

As the presumed mechanism of action authenticates, the anti-cancer agents interact through characteristic binding modes with the DNA of cancer infected cell in such a way that, the cell cannot replicate further. This inhibition of replication finally leads to the death of the infected cell [13]. Especially the coordination complexes are known to perturb the 3D-structure of DNA with the interaction of N-7 nitrogen of nucleotide and hence inhibiting the replication [13]. The detailed SAR studies have rationalized this in terms of labiality and nucleophilicity of ligand and nature of the

metal ion. The inhibitory action of antimicrobial agents is also presumed to follow the same mechanism.

In our laboratory we observed that the pyrazole based transition metal complexes with thiosemicarbazide arms have shown good antibacterial activity as well as strong intercalating interaction with DNA of *Escherichia coli* [14]. It is also envisaged in the literature that the presence of biologically active phenylthiosemicarbazide arms and metal incorporation enhance the activity [15]. By the influence of these results, in continuation, we have developed similar system of different thiosemicarbazide with aromatic substitutions. In this article we wish to report the complexes of a polydentate chelate, architected by incorporating the phenyl thiosemicarbazide fragment at the 3 and 5 positions of a pyrazole core. The thiosemicarbazide arms are expected to provide versatile ligational properties and hence to give stable and interesting transition metal complexes. We made an interaction of this ligand with Co^{II} , Ni^{II} , Cu^{II} and Zn^{II} ions in a 1:2 fashion to get dinuclear, monomeric complexes. The resulted complexes are isolated and characterized spectro-analytically. The prepared compounds are made to interact with *E. coli* DNA and the interaction studies were monitored by absorption, hydrodynamic, thermal denaturation and electrophoresis studies.

2. Materials and methods

2.1. Analysis and physical measurements

All chemicals used were of reagent grade and the solvents were distilled prior to use. The metal estimation was done by standard methods [16]. Carbon, hydrogen, nitrogen, and sulfur analyses

* Corresponding author. Tel.: +91 836 4250821 (R), mobile: +91 9900485652.

E-mail address: vkrevankar@rediffmail.com (V.K. Revankar).

were carried out on a Thermo quest elemental analyzer and the results are represented in Table 1. The molar conductivity measurements in DMF were made on ELICO-CM-82 conductivity bridge with conductivity cell having cell constant 0.51 cm^{-1} . The magnetic susceptibility measurements were made at room temperature using Faraday balance by using $\text{Hg}[\text{Co}(\text{SCN})_4]$ as calibrant. The ^1H NMR spectra were recorded in DMSO-d_6 solvent on Bruker-300 MHz spectrometer at room temperature using TMS as internal reference. IR spectra were recorded in a KBr matrix using Impact-410 Nicolet (USA) FT-IR spectrometer in $4000\text{--}400 \text{ cm}^{-1}$ range. The ESR spectrum of the copper complex was carried out on Varian E-4X-band EPR spectrometer, using TCNE as the g -marker. The FAB mass spectra were drawn from JEOL SX 102/DA-6000 mass spectrometer using Argon/Xenon (6 kV, 10 mA) as the FAB gas and 3-nitrobenzylalcohol as matrix. Thermal studies (Thermo gravimetric and Differential Thermal analysis) were carried out in nitrogen atmosphere on Universal V2.4F TA Instrument with limiting temperature of $1000 \text{ }^\circ\text{C}$ and heating rate $10 \text{ }^\circ\text{C}/\text{min}$. Cyclic voltammetric studies were performed at room temperature in DMF under oxygen free condition created by purging pure nitrogen gas, with CHI1110A Electrochemical analyzer (USA) comprising three electrode assembly of glassy carbon working electrode, platinum auxiliary electrode and Ag^+/AgCl reference electrode. Tetramethylammoniumchloride (0.01 M) was used as supporting electrolyte and instrument was standardized by ferrocene/ferrocenium redox couple. The electronic spectra of the complexes were recorded on Hitachi 150–20 spectrophotometer with scan range of $1000\text{--}200 \text{ nm}$. The same, equipped with temperature controlling thermostat is used for the DNA binding studies (absorption and thermal denaturation studies). Bio-Rad Trans illuminator and a Polaroid camera were used in the gel electrophoresis experiment and Oswald micro-viscometer is used for hydrodynamic measurements.

2.2. Preparation of ligand LH_3 (1-H pyrazole-3,5-dicarboxybis(phenylthiosemicarbazide))

The commercially obtained (Sigma Aldrich) 1H-pyrazole-3,5-dicarboxylic acid (0.01 M) was refluxed with thionylchloride (10 mL) in anhydrous condition for 4 h at about $110\text{--}120 \text{ }^\circ\text{C}$. The content was then evaporated to dryness to remove the excess thionylchloride, thus obtained pasty mass was allowed to cool. Phenylthiosemicarbazide [17] in dry ethanol (0.02 M) was added drop wise and reflux was carried out for additional 3 h. Resultant solution was then cooled in ice bath to get a colorless amorphous solid, which is separated by filtration and dried over anhydrous CaCl_2 and recrystallised from ethanol. The reaction pathway is represented in Fig. 1.

2.3. Preparation of complexes

To the ethanolic solution of the ligand LH_3 (0.454 g, 0.01 M), corresponding metal(II) chloride (0.02 M) in ethanol was added with stirring and refluxed on water bath for 4 h. So obtained solid complex was separated by filtration under suction, washed with hot ethanol and dried in *vacuo*.

Table 1
Elemental analysis and conductivity data of compounds.

Compound	Empirical formula	Elemental analysis in% calculated (found)						Molar cond. A_M in $\text{ohm}^{-1} \text{ cm}^2 \text{ mol}^{-1}$
		C	H	N	M	S	Cl	
LH_3	$[\text{C}_{19}\text{H}_{18}\text{N}_8\text{S}_2\text{O}_2]$	50.21 (50.12)	3.99 (3.83)	24.65 (24.58)	–	14.12 (14.23)	–	–
CoL	$[\text{Co}_2\text{L}(\mu\text{OH})(\text{H}_2\text{O})_4]$	34.71 (34.82)	3.53 (3.62)	17.05 (17.14)	17.93 (18.12)	9.74 (9.63)	–	15.2
NiL	$[\text{Ni}_2\text{L}(\mu\text{OH})(\text{H}_2\text{O})_4]$	34.75 (34.64)	3.51 (3.62)	17.07 (17.16)	17.83 (17.78)	9.75 (9.86)	–	11.4
CuL	$[\text{Cu}_2\text{L}(\mu\text{Cl})(\text{H}_2\text{O})_4]$	33.32 (33.45)	3.21 (3.30)	16.37 (16.22)	18.56 (18.92)	9.35 (9.53)	5.11 (5.23)	14.0
ZnL	$[\text{Zn}_2\text{L}(\mu\text{Cl})(\text{H}_2\text{O})_4]$	33.14 (33.27)	2.61 (2.82)	16.28 (16.23)	19.02 (19.54)	9.30 (9.42)	5.08 (5.18)	12.9

2.4. DNA binding/cleavage studies

2.4.1. Isolation of DNA *E. coli*

Nutrient broth peptone (10 g/L), Yeast extract (5 g/L) and (NaCl 10 g/L) were used for culturing of *E. coli*. The 50 mL media was prepared, autoclaved for 15 min at $121 \text{ }^\circ\text{C}$, 15 lb pressure. The autoclaved media were inoculated with the seed culture and incubated at $37 \text{ }^\circ\text{C}$ for 24 h for *E. coli*. The fresh bacterial culture (1.5 mL) was centrifuged to obtain the pellet and was dissolved in 0.5 mL of lysis buffer (100 mM tris pH 8.0, 50 mM EDTA, 10% SDS) and to which 0.5 mL of saturated phenol was added and incubated at $55 \text{ }^\circ\text{C}$ for 10 min. The incubated solution was centrifuged at 10,000 rpm for 10 min and to the supernatant an equal volume of chloroform, isoamyl alcohol (24:1) and 1/20th volume of 3 M sodium acetate (pH 4.8) were added. The mixture was again centrifuged at 10,000 rpm for 10 min and to the supernatant 3 volumes of chilled absolute alcohol was added. The precipitated DNA was separated by centrifugation and dried and dissolved in TE buffer (10 mM tris pH 8.0, 1 mM EDTA) and stored in cool.

The concentration of DNA per nucleotide $[\text{C}(\text{p})]$ was measured by using its known extinction coefficient at 260 nm ($\sim 6600 \text{ M}^{-1} \text{ cm}^{-1}$) [18]. The absorbance at 260 nm (A_{260}) and at 280 nm (A_{280}) for DNA was measured to check its purity. The ratio A_{260}/A_{280} was found to be 1.88, indicating that DNA was satisfactorily free from protein [19]. Tris buffer [5 mM tris (hydroxymethyl) aminomethane, tris, pH 7.2, 50 mM NaCl] was used for the absorption, viscosity, and thermal denaturation experiments.

2.4.2. Absorption studies

The complexes were dissolved in DMSO and then diluted to the desired concentration with distilled water. The spectroscopic titrations were carried out by adding increasing amounts of DNA to a solution of the complex at a fixed concentration contained in a quartz cell. After each addition, the UV-Visible spectra were recorded after equilibration at $20 \text{ }^\circ\text{C}$ for 10 min. The intrinsic binding constant K_b was determined from the plot of $A_0/[A - A_0]$ vs $[\text{DNA}]^{-1}$ according to equation [20]

$$A_0/[A - A_0] = \varepsilon_G/[\varepsilon_{\text{H-G}} - \varepsilon_G] + \varepsilon_G/[\varepsilon_{\text{H-G}} - \varepsilon_G] \times 1/K[\text{DNA}]$$

where A_0 – absorbance in the free complex; A – absorbance at given DNA concentration; $[\text{DNA}]$ – concentration of DNA in base pairs; ε_G – the apparent absorption coefficients of DNA in free form; $\varepsilon_{\text{H-G}}$ – the apparent absorption coefficients of DNA in bounded form of complex. The data were fitted to above equation and graph was obtained with a slope equal to $\varepsilon_G/[\varepsilon_{\text{H-G}} - \varepsilon_G] \times 1/K$ and intercept equal to $\varepsilon_G/[\varepsilon_{\text{H-G}} - \varepsilon_G]$. Hence K_b was obtained from the ratio of the intercept to the slope.

2.4.3. Hydrodynamic measurements (viscosity measurements)

Viscosity measurements were carried out using an Oswald micro-viscometer maintained at constant temperature ($20 \text{ }^\circ\text{C}$) in a thermostat bath. The complexes were dissolved in DMSO and then diluted to the desired concentration with distilled water. The DNA concentration was kept constant in all samples (100 μM), but the complex concentration was increased each time (from 20 to

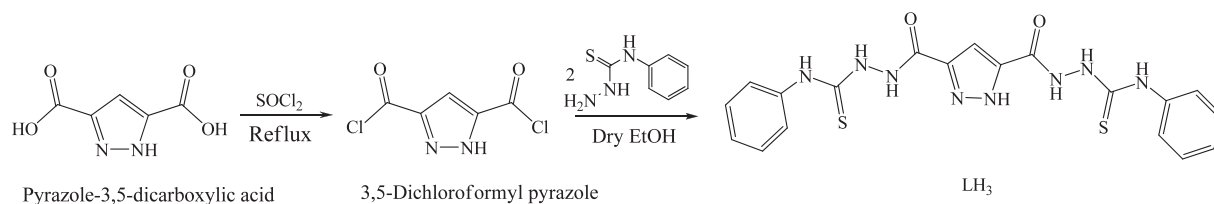


Fig. 1. Schematic representation of preparation of ligand LH₃.

80 μM). Mixing of the solution was achieved by bubbling the nitrogen gas through viscometer. The flow time was measured with a digital stopwatch. The sample flow times were measured three times and the mean value was used. Data are presented in plot of $(\eta/\eta_0)^{1/3}$ versus the ratio $[\text{complex}]/[\text{DNA}]$, where η and η_0 are the specific viscosity of DNA in presence and in absence of the complex respectively. The values of η and η_0 were calculated by using equation [21]

$$\eta = (t - t_0)/t_0$$

where t – the observed flow time of DNA containing solution; t_0 – the flow time of DNA solution alone.

Relative viscosities for DNA were calculated from the relation (η/η_0) .

2.4.4. Thermal denaturation study

Thermal denaturation studies were carried out on UV-spectrometer equipped with temperature controlling thermostat. The melting curves (T_m -curve) of both free *E. coli* DNA and DNA bound complexes were obtained by measuring the hyperchromicity of DNA at 260 nm as a function of temperature. The melting temperatures were measured with 60 μM DNA in phosphate buffer at pH 6.8 ($\mu = 0.2 \text{ M NaCl}$). The temperature was scanned from 25 to 85 $^\circ\text{C}$ at a rate of 5 $^\circ\text{C}$ per min. The mid-point of the hyperchromic transition was noted as the melting temperature (T_m) [22].

2.4.5. Electrophoresis

For the gel electrophoresis experiments [23], the solution of complexes in DMF (1 mg/mL) was prepared and these test samples (1 μg) were added to the genomic DNA samples of *E. coli* and incubated for 2 h at 37 $^\circ\text{C}$. Agarose gel was prepared in TAE buffer (4.84 g Tris base, pH 8.0, 0.5 M EDTA/l. pH 7.3), the solidified gel attained at ~ 55 $^\circ\text{C}$ was placed in electrophoresis chamber flooded with TAE buffer. After that 20 μL of each of the incubated complex-DNA mixtures (mixed with bromophenol blue dye at 1:1 ratio) was loaded on the gel along with standard DNA marker and electrophoresis was carried out under TAE buffer system at 50 V for 2 h. At the end of electrophoresis, the gel was carefully stained with EtBr (ethidiumbromide) solution (10 $\mu\text{g}/\text{mL}$) for 10–15 min and visualized under UV light using a Bio-Rad Trans illuminator. The illuminated gel was photographed by using a Polaroid camera (a red filter and Polaroid film were used).

3. Results and discussion

3.1. Molar conductivity measurements

The molar conductance values of all the complexes measured at room temperature in DMF solution with $10^{-3} \text{ mol dm}^{-3}$ concentration fall in the range 11.4–15.2 $\text{mho cm}^2 \text{ mol}^{-1}$, which indicate the non-electrolytic nature of the complexes [24].

3.2. Infrared spectral analysis

IR spectrum of ligand shows sharp absorptions around 3200 cm^{-1} attributed to $\nu(-\text{NH})$. A strong band at 1665 cm^{-1} is

assigned to amide carbonyl stretching vibration and band around 1540 cm^{-1} is assigned to pyrazole ring $\nu(\text{C}=\text{N})$. The thione ($\text{C}=\text{S}$) form of ligand is suggested by the thioamidic absorptions observed around 1291 cm^{-1} and 788 cm^{-1} [25]. Upon complexation the peak corresponding to $\nu(\text{C}=\text{O})$ disappears by providing a new band around 1620 cm^{-1} assignable to $\nu(\text{C}=\text{N})$, which suggests the possible imidol formation and coordination of ligand through azomethine nitrogen. Appearance of a sharp band in the region 3400 cm^{-1} attributable to the $\nu(-\text{OH})$ supports the same. Pyrazole ring nitrogens are involved in ligation as diazene bridge, which is suggested by the high frequency shift of ring $\nu(\text{C}=\text{N})$ and presence of $\nu(\text{M}-\text{N})$ around 465 cm^{-1} . It is seen that thioamidic bands that have major contribution from $\text{C}=\text{S}$ group are disappeared in complexes suggesting the thioenolisation, which is supported by the appearance of $\nu(\text{C}-\text{S})$. The absence of $\nu(-\text{SH})$ allow us to conceive the sulfur coordination upon deprotonation, which is further supported by the presence of $\nu(\text{M}-\text{S})$ band in the complexes. Sharp band at 3550 cm^{-1} in the Co^{II} and Ni^{II} complexes evidences the μOH and presence of coordinated water molecules broaden the higher wavelength side of spectra. The numerical IR spectral data is tabulated (Table 2).

3.3. ^1H NMR spectral studies

^1H NMR study of the ligand and Zn^{II} complex was carried out in the scan range of 0–16 δppm . The ligand displayed a sharp singlet peak at 12.03 δppm which is attributable to N–H proton of pyrazole [26]. Disappearance of the same in the complex reveals the formation of pyrazolide ion and coordination of pyrazole as endogenous bridge. In ligand, amide protons are resonated at 10.63 δppm and disappeared upon complexation evidencing the enolisation process, which is attested by the peak due to $-\text{OH}$ at 11.63 δppm . The thioamidic protons assigned at 10.16 δppm were disappeared in the complex suggesting the thioenolisation and subsequent deprotonation. The aromatic and phenyl amine protons resonated around 7–8 δppm and 8.3 δppm respectively experience a small shift in complex due to the changed electronic environment brought about by the chelation. Further the appearance of broad peak at around 3.4 δppm reveals the presence of coordinated water in the complex.

3.4. UV-Visible spectral studies

The electronic spectra of ligand and complexes were recorded in DMF solution in the scan range 200–1000 nm. Ligand exhibits a band around 270 nm which is due to the intra ligand $\pi \rightarrow \pi^*$ transition, which is unaltered in spectra of complexes. The peak at 320 nm is assigned for $n \rightarrow \pi^*$ transition of imine group and the transitions occurred around 275–300 are due to $n \rightarrow \pi^*$ transitions of carbonyl group [27]. In cobalt complex, the band around 390 nm is assigned to LMCT, $n \rightarrow \pi^*$ transition. The band at 450 and 644 nm are attributed to $d \rightarrow d$ transitions, which are represented as $^4\text{T}_{1g} \rightarrow ^4\text{A}_{2g}$ and $^4\text{T}_{1g} (\text{F}) \rightarrow ^4\text{T}_{1g} (\text{P})$ assigning the octahedral structure. In Ni^{II} complex the lowest energy band observed at 900 nm was due to $^3\text{A}_{2g} \rightarrow ^3\text{T}_{2g}(\nu_1)$ and bands at 600 and 440 nm were assigned to $^3\text{A}_{2g} \rightarrow ^3\text{T}_{1g}(\nu_2)$ and $^3\text{A}_{2g} \rightarrow ^3\text{T}_{2g}(\text{P})(\nu_3)$ respectively, suggesting the octahedral geometry. The copper complex

Table 2
Infrared spectral data of ligand and its complexes in cm^{-1} (s – sharp, m – medium and b – broad).

Compound	$\nu(\mu\text{OH})$	$\nu(\text{O}-\text{H})$	$\nu(\text{N}-\text{H})$	$\nu(\text{N}-\text{H})$ pyrazole	$\nu(\text{C}=\text{O})$ amide	$\nu(\text{C}=\text{N})$	$\nu(\text{C}=\text{N})$ pyrazole	$\nu(\text{C}=\text{S})$ thioamide	$\nu(\text{C}-\text{S})$	$\nu(\text{M}-\text{N})$	$\nu(\text{M}-\text{S})$	
LH ₃	–	–	3286m	3176s	1665s	–	1540	1291s	788s	–	–	
CoL	3561m	3350b	3227m	–	–	1622s	1550s	–	–	658m	468s	420s
NiL	3550m	3340b	3230m	–	–	1620s	1578s	–	–	653m	468s	416s
CuL	–	3342b	3220m	–	–	1625s	1560m	–	–	649s	469m	418s
ZnL	–	3346b	3215m	–	–	1621s	1551s	–	–	662s	476s	412s

exhibit band around 650 nm with low ϵ value, which is absent in zinc complex, is assigned to $d \rightarrow d$ transition. The intense band observed at 480 nm is referred for ligand to metal charge transfer transition (LMCT). The electronic spectrum of zinc complex shows band at 350 nm, accounted for the intra ligand and LMCT transitions.

3.5. Magnetic properties

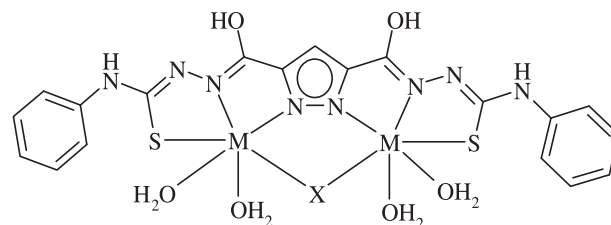
The copper complex exhibits the effective magnetic moment μ_{eff} 1.64 BM at 303 K. Fairly low value obtained evidences the existence endogenous pyrazole bridge with possible spin–spin interaction. The room temperature magnetic moment values of bis-complexes of nickel and cobalt complexes were found to be 2.78 and 4.26 BM respectively, suggesting the six coordinated distorted octahedral geometry [28,29], which is in line with the spectral analysis data.

3.6. ESR spectral study

The X-band ESR spectrum of Cu^{II} complex in solid form scanned in the region of 9000 MHz with corresponding field intensity of ~ 3000 Gauss exhibits isotropic intense broad signal with $g_{\text{iso}} = 2.075$ with no hyperfine splitting. This type of unusual ESR spectrum was assigned for complexes having large organic ligand substitutions with exogenous chloro bridge. The broadening in signal is may be attributed to the existence of dipolar interaction in the complex. Further broadening of signal suggests alike chemical environment for both copper ions [26,30].

3.7. FAB mass spectral studies

The spectral and analytical data suggests the empirical formula $[\text{M}_2\text{L}(\mu\text{Cl})(\text{H}_2\text{O})_4]$ for the copper complex, this is supported by the



For $\text{M} = \text{Co}$ and Ni , $\text{X} = \text{OH}$
for $\text{M} = \text{Cu}$ and Zn , $\text{X} = \text{Cl}$

Fig. 2. Structures of complexes.

FAB mass spectra. The peaks at highest m/z value can be assigned for molecular mass by certainty, with the aid of consistent isotopic pattern. A peak at m/z 721 was observed, in the Cu^{II} complex which is in consistent with the total molecular mass of the coordination complex (Fig. 3). Apart from this, spectrum shows some other peaks, which are due to molecular cations of various fragments of complex. By comparing the analytical and spectral data of cobalt, nickel and zinc complexes, it is evident that these are monomeric and binuclear complexes. The tentative structure assigned for the complexes is represented as Fig. 2.

3.8. Thermal studies

The thermal stability and decomposition pattern of the complexes was analyzed by TG and DTA studies. Thermo gravimetric analysis of the complexes has been carried out in nitrogen atmosphere with heating rate of $10^\circ\text{C}/\text{min}$.

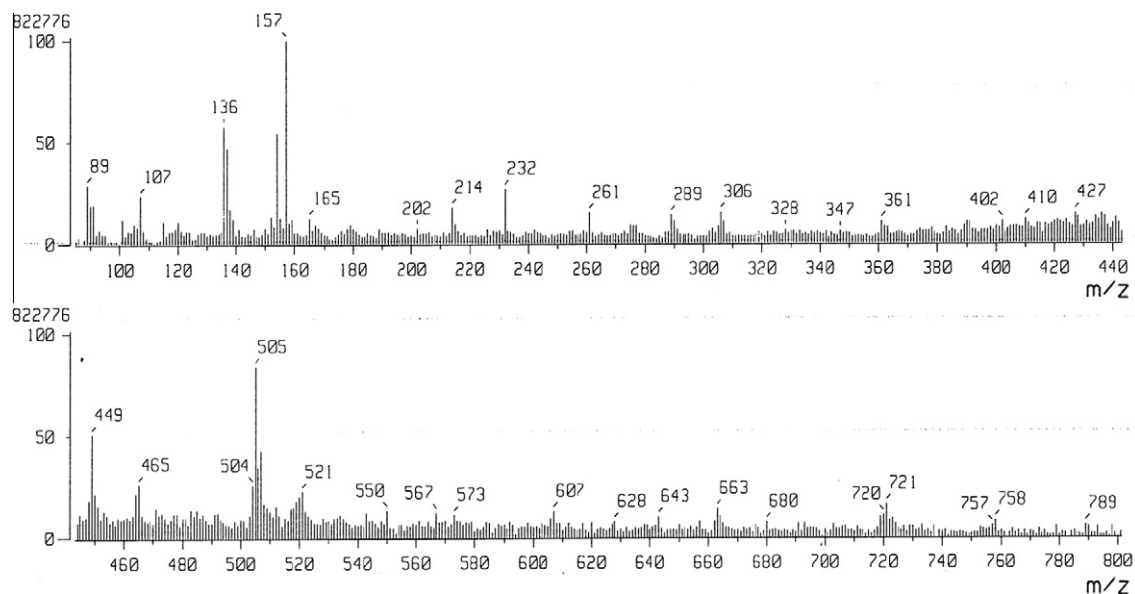


Fig. 3. FAB mass spectrum of the copper complex, $[\text{Cu}_2\text{L}(\mu\text{Cl})(\text{H}_2\text{O})_4]$.

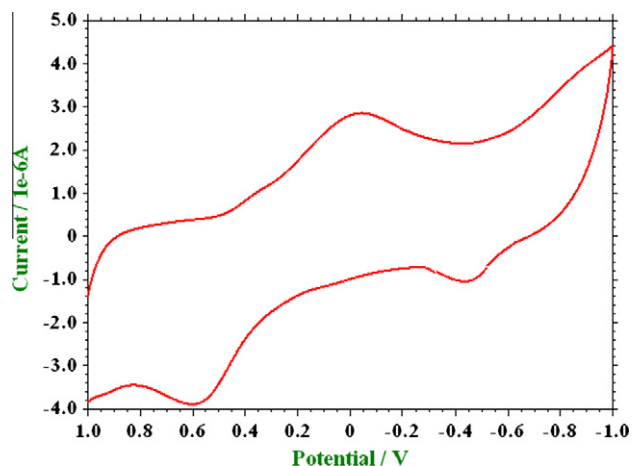


Fig. 4. Cyclic voltammogram of $[Cu_2L(\mu Cl)(H_2O)_4]$ with scan rate 0.1 V/s.

It is observed that in the present copper complex, decomposition takes place in two stages. The first step of decomposition corresponds to a mass loss of $\sim 9.98\%$ in the range $120\text{--}150\text{ }^\circ\text{C}$ is attributed to the loss of four coordinated water molecule. The corresponding DTA peak at $\sim 137\text{ }^\circ\text{C}$ signifies the endothermic process. Second stage of mass loss of 13.57% taking place at the range $200\text{--}250\text{ }^\circ\text{C}$ with respective DTA curve at $\sim 220\text{ }^\circ\text{C}$ representing the exothermic process, corresponds to the decomposition of ligand. The final product was analyzed to be metal oxide.

3.9. Cyclic voltammetric studies

The ligand and complexes (0.001 M in DMF) were scanned in the potential range of -1.0 V to 1.0 V in deaerated condition with different scan rates (0.05, 0.1 and 0.15 V/s). The ligand and other complexes do not show electrochemical response in the applied range revealing that the redox property exhibited by the copper complex is purely metal based. The voltammogram with scan rate 0.1 V/s is given in Fig. 4 and numerical results are represented in Table 3. A cathodic peak observed in the voltammograms in the range $E_{pc} = -0.05$ to -0.14 V evidences the reduction of metallic species, $Cu^{II} \rightarrow Cu^I$. The reverse scan shows two anodic peaks with potentials in the range, $E_{pa_1} = -0.35$ to -0.45 V and $E_{pa_2} = 0.55$ to 0.61 V corresponding to the oxidation reactions, $Cu^I \rightarrow Cu^{II}$ and $Cu^{II} \rightarrow Cu^{III}$.

Table 3
Cyclic voltammetry results.

Complex	Scan rate (V/s)	E_{pc} (V)	E_{pa} (V)	ΔE_p (V)	$E_{1/2}$ (V)	I_{pc}/I_{pa}
CuL	0.15	-0.05	-0.45	0.52	0.40	-0.25
	0.1	-0.1	-0.40	0.58	0.30	-0.25
	0.05	-0.14	-0.35	0.61	0.21	-0.24

$$\Delta E_p = E_{pa_1} - E_{pc}; E_{1/2} = [E_{pc} + E_{pa_1}]/2.$$

Table 4
Analysis of antibacterial activity.

Compound	500 μg				250 μg			
	<i>E. coli</i>		<i>Pseudomonas aeruginosa</i>		<i>E. coli</i>		<i>Pseudomonas aeruginosa</i>	
	Zone of inhibition in cm	% of inhibition	Zone of inhibition in cm	% of inhibition	Zone of inhibition in cm	% of inhibition	Zone of inhibition in cm	% of inhibition
Gentamycine	3.2	100	2.9	100	3.0	100	2.4	100
LH ₃	0.8	25.00	0.8	27.58	0.6	20.00	0.5	20.83
CoL	1.1	34.37	1.0	34.48	0.9	30.00	0.7	29.16
NiL	2.2	68.75	1.6	55.17	1.8	60.00	1.3	54.16
CuL	3.4	106.2	2.5	86.20	3.0	100	2	8.33
ZnL	1.4	43.75	1.2	41.37	1.2	40.00	0.8	33.34
DMF	0.1	3.12	-	-	-	-	-	-

The high value of ΔE_p , separation between the cathodic and anodic peak potentials ($E_{pa} - E_{pc}$) for the couple Cu^I/Cu^{II} which is greater than 60 mV indicate the quasi-reversible nature of the redox process [31]. The dependency of peak potentials on scan rate and almost constant values of I_{pc}/I_{pa} , peak current ratio (~ 1), which are the characteristic features for quasireversible process, are observed in the present study supporting the presumed nature of redox process. The electrochemical activity of copper complex and its quasireversible nature can be explained in terms of flexibility and the size of the coordination cavity in the complexes and the geometric requirements and the size of the metal ions in the different oxidation states [32]. Further detailed studies are required to understand the nature of chemical reactions following the electron transfers which are helpful in enzyme catalysis.

3.10. Anti biogram analysis of the compounds against fungi and bacteria

The comparative biological activities were studied by screening the ligand and its complexes antibacterial and antifungal activity against gram negative bacteria *E. coli*, *Pseudomonas aeruginosa* and fungi *Aspergillus niger*, *Cladosporium* at 500 μg and 250 μg (in DMF) concentrations using cup-plate method. Gentamycine and Flucanazol were used as standards for bacteria and fungi respectively. Out of above concentrations the later is treated as minimum inhibitory concentration (MIC). The data is summarized in Tables 4 and 5 and the same is represented graphically in Figs. 5 and 6. Ligand is found to be moderately active against bacteria *E. coli*, *P. aeruginosa* and fungus *A. niger* and show mild inhibition in case of fungus *Cladosporium*. A definite enhancement in the activity of compound is observed upon complexation, which is illustrated graphically. The cobalt and zinc complexes show moderate activity against all microorganisms, which is appreciable as compared to the ligand where as the nickel complex shows better activity against bacteria and moderate activity against fungi. The copper complex shows very good (as good as the internal standard) activity against *E. coli* and comparatively good activity against *P. aeruginosa* and both the fungi. This enhancement in antimicrobial property, which is brought about upon complexation can be related to the increased lipophilicity which powers the rate of entry of molecules into the cell and inertness of certain metal ligand linkages which protects the molecule against enzymatic degradation.

Table 5
Analysis of the antifungal activity.

Compound	500 µg				250 µg			
	<i>A. niger</i>		<i>Cladosporium</i>		<i>A. niger</i>		<i>Cladosporium</i>	
	Zone of inhibition in cm	% of inhibition	Zone of inhibition in cm	% of inhibition	Zone of inhibition in cm	% of inhibition	Zone of inhibition in cm	% of inhibition
Flucanazole	1.2	100	0.9	100	1.0	100	0.8	100
LH ₃	0.3	25.00	0.2	22.23	0.1	10.00	–	–
CoL	0.4	33.34	0.3	33.34	0.2	20.00	0.1	12.50
Nil	0.5	41.66	0.4	44.45	0.4	40.00	0.3	37.50
CuL	0.8	66.67	0.5	55.56	0.6	60.00	0.4	50.00
ZnL	0.5	41.66	0.3	33.34	0.3	30.00	0.1	12.50
DMF	–	–	–	–	–	–	–	–

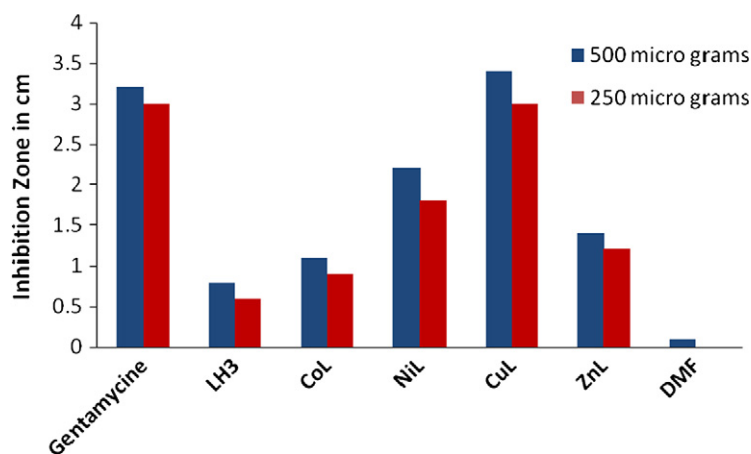
The compounds have exhibited the higher inhibitory action against bacterium, *E. coli*. Hence to investigate the applicability of the said mechanism, the *in vitro* interaction studies of compounds with *E. coli* DNA were carried out.

3.11. DNA binding/cleavage studies

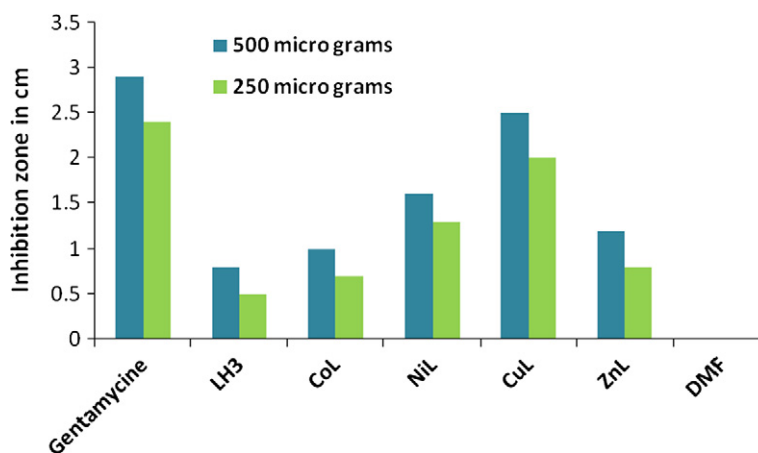
3.11.1. Absorption studies

In the present investigation the binding of ligand and its metal complexes (500 µM) with *E. coli* DNA, in different concentrations (50–200 µM) has been characterized classically through absorption spectral titrations by following the changes in absorbance and shift in the wavelength as a function of added concentration of DNA.

In the case of copper complex (Fig. 7) the broad intense band at 480 nm assigned to LMCT is monitored as a function of added DNA. Observations made reveal that increase in amount of DNA results the decrease in molar absorptivity (hypochromism) as well as red shift of ~16 nm (bathochromic shift) which indicate the intercalative mode of interaction of complex with DNA [33]. The intrinsic binding constant K_b determined by the plot of $A_0/[A - A_0]$ vs $[DNA]^{-1}$ with value $1.25 \times 10^4 M^{-1}$, which is good as compared with the classical intercalators ($K_b \sim 10^6$) suggest the moderate intercalative interaction [34]. In the case of ligand and other complexes similar behavior is observed but with low hypochromism and insignificant red shift. This suggests the low binding capacity of the compounds which is evidenced by the magnitude of intrinsic



a. *Escherichia coli*



b. *Pseudomonas aeruginosa*

Fig. 5. Graphical representation of antibacterial analysis of the ligand and complexes.

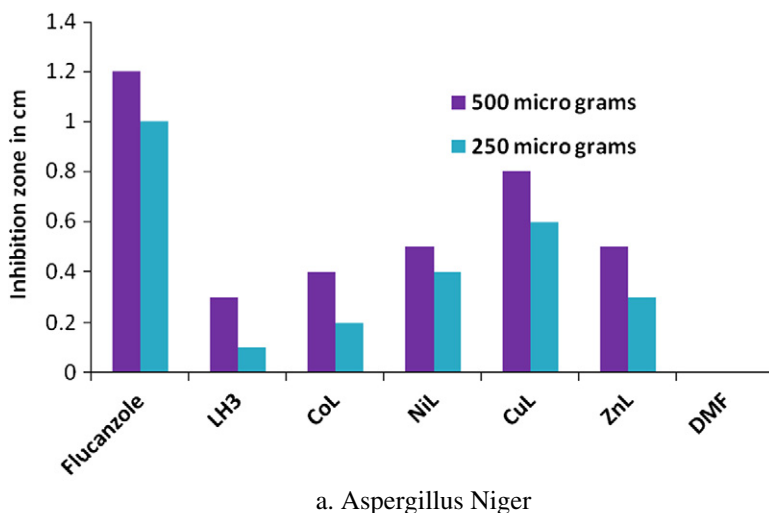
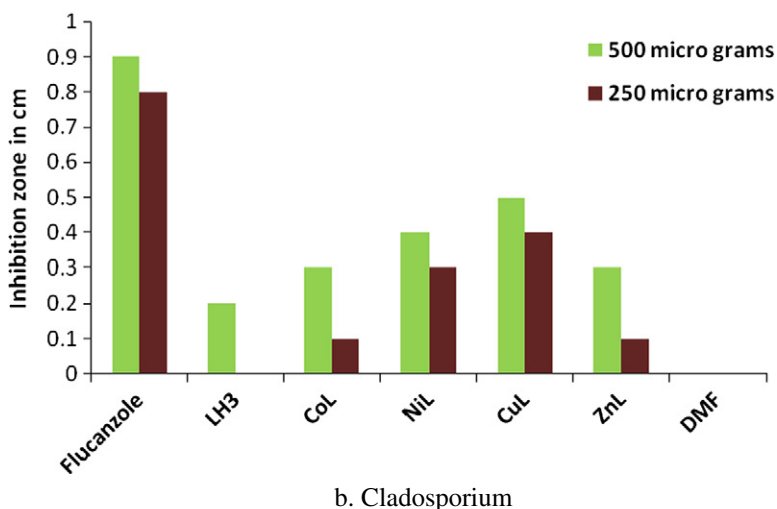
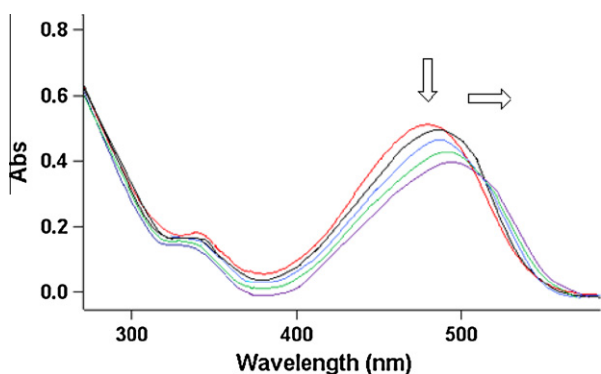
a. *Aspergillus Niger*b. *Cladosporium*

Fig. 6. Graphical representation of antifungal activity of ligand and complexes.

Fig. 7. Absorption spectrum of $[\text{Cu}_2\text{L}(\mu\text{Cl})(\text{H}_2\text{O})_4]$ showing the variation of absorption with respect to the increase in the DNA concentration.

binding constants obtained, i.e., $K_b = 9.8 \times 10^3 \text{ M}^{-1}$, $6.8 \times 10^3 \text{ M}^{-1}$, $7.3 \times 10^3 \text{ M}^{-1}$ and $4.5 \times 10^3 \text{ M}^{-1}$ for nickel, cobalt, zinc complexes and ligand respectively.

A majority reports indicate that the presence of labile ligand units, play a vital role in the DNA binding strategy of metal complexes. Effectiveness of the DNA binding/cleavage depends on the nucleophilic nature of the labile ligand attached to the metal centers and the nature of metal ion itself. In the present complexes the architecture of ligand is so that it provides at least one labile ligand

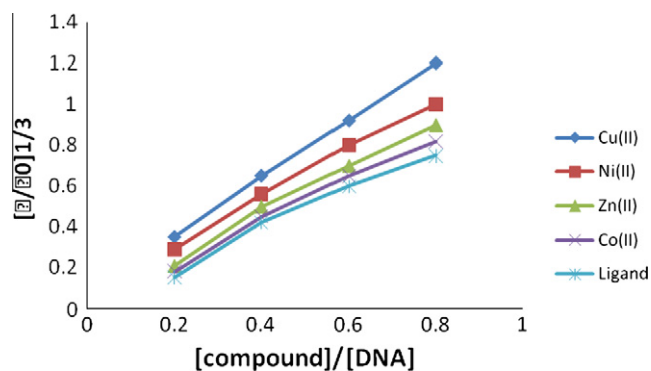


Fig. 8. Effect of added compound with increasing concentration on the viscosity of DNA at 20 °C.

viz., chloride/hydroxyl group, which is responsible for the interaction of the compounds with N-7 of nucleotide, which leads to the perturbation of DNA structure and hence inhibiting the replication. The higher DNA binding ability of copper complex, in particular can be assigned to its biocompatibility, high nucleobase affinity and capacity to possess biologically accessible redox potentials. It can recognize nucleic acids, in a sequence-specific fashion and bind to them in such a way that their functioning will be altered [35].

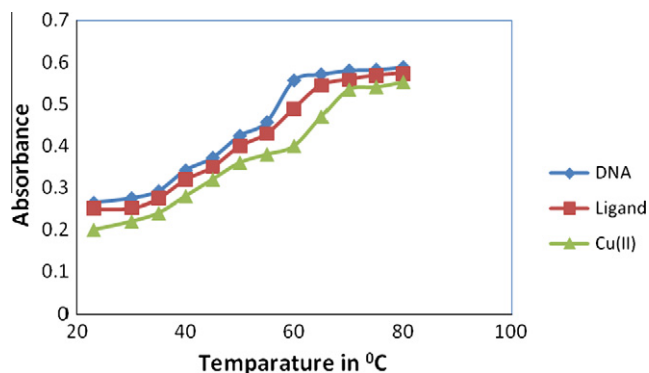


Fig. 9. Effect of added complexes on the melting temperature (T_m) of *E. coli* DNA.

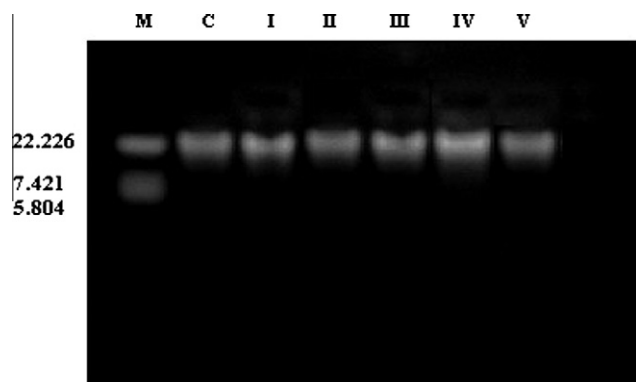


Fig. 10. Photograph showing the effects of metal complexes on DNA of *E. coli*. Lane M: DNA marker, Lane C: Untreated DNA, Lane I: Ligand (LH_3), Lane II: $[Co_2L(\mu OH)(H_2O)_4]$, Lane III: $[Ni_2L(\mu OH)(H_2O)_4]$, Lane IV: $[Cu_2L(\mu Cl)(H_2O)_4]$, Lane V: $[Zn_2L(\mu Cl)(H_2O)_4]$.

3.11.2. Viscometric measurements

This is one of the most critical tests for inferring the binding mode (intercalation or other binding modes) of DNA in solution and was regarded as the least ambiguous and the most critical test of binding mode in solution in the absence of crystallographic structural data. Intercalation of drugs like ethidium bromide causes a significant increase in the viscosity of DNA solutions due to increase in the separation of base pairs at intercalation sites and hence increase in overall DNA contour length. By the other hand, molecules that bind exclusively in the DNA grooves typically cause less pronounced (positive or negative) or no changes in the DNA solution viscosity. As a means for further exploring the binding of present ligand and complexes, viscosity measurements were carried out on solution of *E. coli* DNA (100 μM) by varying the concentration of added compounds (20–80 μM) under appropriate conditions. The values of $(\eta/\eta_0)^{1/3}$ obtained, where η and η_0 are the specific viscosity of DNA in presence and in absence of the complex respectively were plotted against $[compound]/[DNA]$ (Fig. 8). The results reveal that all the complexes and ligand that are bound to *E. coli* DNA show increase in relative viscosities with an increase in the $[compound]/[DNA]$ ratio suggesting the intercalative binding mode of the compounds with DNA [20], which is in line with the results obtained from absorption studies. Change in viscosity caused by the copper complex was more evident than by others, which indicate the strong intercalating capacity of complex.

3.11.3. Thermal denaturation studies

Information about the interaction strength of complexes with DNA is offered by thermal behaviors of DNA in the presence of complexes. It is known that when the temperature of solution

increases, the double stranded DNA gradually dissociates to single strands and generates a hyperchromic effect on the absorption spectra of DNA bases ($\lambda_{max} = 260$ nm). In order to identify this transition process, the melting temperature T_m , which is defined as the temperature where half of the total base pairs are unbound, is introduced. According to the literature the interaction of natural or synthesized organics and metallointercalators generally results in a considerable increase in melting temperature. Hence the DNA melting experiment is useful in establishing the extent of intercalation binding between the compound and DNA. The T_m of *E. coli* DNA in the absence of any added complex was found to be 58 ± 1 °C in our experimental conditions. Under the same set of conditions, the presence of all the complexes has increased the T_m . The copper complex show hypochromicity with increased T_m of 64 ± 1 °C ($\Delta T_m = 5$ °C) which is characteristic of intercalative binding behavior (Fig. 9) [21]. The ligand though shows hypochromicity and shift of T_m for 2–3 °C, but the extent is less as compared to the copper complex. Which suggest the mild intercalation of ligand with DNA. All other complexes show little variation in T_m and decrease in absorbance with values falling in between the copper complex and the ligand. The results obtained by the hydrodynamic and absorbance studies are well supported by the thermal denaturation experiment.

3.11.4. Gel electrophoresis method

After binding to DNA, duly designed metal complexes can induce several changes in DNA conformation. Metal complexes, which could induce DNA deformations, such as bending, 'local denaturation' (overwinding and underwinding), intercalation, micro loop formation and subsequent DNA shortening lead to decrease in molecular weight of DNA. Gel electrophoresis is an extensively used technique for the study binding of compounds with nucleic acids; in this method segregation of the molecules will be on the basis of their relative rate of movement through a gel under the influence of an electric field. DNA is negatively charged and when it is placed in an electric field, it migrates towards the anode; the extent of migration of DNA is decided by the strength of electric field, buffer, density of agarose gel and size of the DNA. Generally it is seen that mobility of DNA is inversely proportional to its size. Gel electrophoresis picture is shown in Fig. 10. The photograph shows the bands with different bandwidth and brightness compared to the control. The difference observed in the intensity and the band width is the criterion for the evaluation of binding/cleavage ability of ligand and its transition metal complexes with DNA of *E. coli*. Unaided DNA does not show any significant cleavage of DNA even after a longer exposure time in Lane-C, representing Control experiment. There is no significant binding/cleavage of DNA is taking place by means of ligand and Co^{II} complex which has been indicated by the intensity and the mobility (tailing) of lane-I and II, which are found to be as same as the control band. In lane III and V width of the DNA band is enlarged due to the tailing and shows little increase in intensity, which may be attributed to the binding of Ni^{II} and Zn^{II} complexes to the DNA for small extent. The high intensity band with maximum tailing in lane IV suggests the strong binding of Cu^{II} complex to the DNA. From the above observation it has been concluded that the intercalative binding of the metal complexes caused a change in the conformation of DNA [36].

4. Conclusion

It is concluded from analytical and spectral data that, the ligand acts as hexadentate tribasic chelate with N_4S_2 donating sites. All the complexes are non-electrolytic in nature. Electronic and magnetic moment data witnessed the octahedral geometry around the metal ions. Only Cu^{II} complex showed electrochemical activity

in the applied potential range where as ligand and other complexes are found to be electrochemically innocent. Ligand possesses significant activity against microbes which is further enhanced upon complexation. The observations made in DNA binding study of ligand and its complexes interacting with *E. coli* DNA reveal the moderate intercalative mode of interaction of the compounds which may be the cause of their antimicrobial activity. The Cu^{II} complex has exhibited higher binding ability with DNA which is correlated to the significant antimicrobial activity exhibited by the complex.

Acknowledgments

The authors thank Department of chemistry and USIC, Karnatak University, Dharwad for providing spectral and analytical facility. Recording of FAB mass spectra (CDRI Lucknow), ESR spectrum (IIT Bombay) are gratefully acknowledged. The authors (NVK, AK and SB) thank Karnatak University, Dharwad and University Grant Commission for providing the Nilekani Scholarship and RFSMS.

References

- [1] H.D. Hollis Showalter, J.L. Johnson, J.M. Hoftiezer, W.R. Turner, L.M. Werbel, W.R. Leopold, J.L. Shillis, R.C. Jackson, E.F. Elslagert, *J. Med. Chem.* 30 (1987) 121–131; S.A.F. Rostom, M.A. Shalaby, M.A. El-Demellawy, *Eur. J. Med. Chem.* 38 (2003) 959–974.
- [2] A.K. Tewari, A. Mishra, *Bioorg. Med. Chem.* 9 (2001) 715–718.
- [3] R.H. Wiley, P. Wiley, *Pyrazolones, Pyrazolidones and Derivatives*, John Wiley and Sons, New York, 1964.
- [4] S.L. Janus, A.Z. Magdif, B.P. Erik, N. Claus, *Monatsh. Chem.* 130 (1999) 1167–1174.
- [5] V. Michon, C.H. Du Penhoat, F. Tombret, J.M. Gillardin, F. Lepage, L. Berthon, *Eur. J. Med. Chem.* (1995) 147–155.
- [6] I. Yildirim, N. Ozdemir, Y. Akçamur, M. Dinçer, O. Andaç, *Acta Crystallogr.* 61 (2005) 256–258.
- [7] D.M. Bailey, P.E. Hansen, A.G. Hlavac, E.R. Baizman, J. Pearl, A.F. Defelice, M.E. Feigenson, *J. Med. Chem.* 28 (1985) 256–260.
- [8] C.K. Chu, J. Cutler, *J. Heterocycl. Chem.* 23 (1986) 289–319.
- [9] M.R. Grimmett, in: D. Barton, W.D. Ollis (Eds.), *Obshchaya Comprehensive Organic Chemistry*, vol. 8, Pergamon, Oxford, 1979.
- [10] M. Munakata, L.P. Wu, M. Yamamoto, T. Kuroda-Sowa, M. Maekawa, S. Kawata, S. Kitagawa, *J. Chem. Soc. Dalton Trans.* (1995) 4099–4106.
- [11] T.C. Schenck, J.M. Dowens, C.R.C. Milne, P.B. Mackenzie, H. Boucher, J. Whelan, B. Bosnich, *Inorg. Chem.* 24 (1985) 2334–2337.
- [12] F. Meyer, A. Jacobi, B. Nuber, P. Rutsch, L. Zsolnai, *Inorg. Chem.* 37 (1998) 1213–1218; A.J. Vincent, M. Kumar, M. Jose, L. Laurent, N. Pilar, G.E. Espana, R.A. Jose, L.V. Santiago, E. Beatriz, *J. Org. Chem.* 64 (1999) 6135–6146.
- [13] S.E. Sherman, S.J. Lippard, *Chem. Rev.* 87 (1987) 1153–1181.
- [14] N.V. Kulkarni, V.K. Revankar, *J. Coord. Chem.* 64 (2011) 725–741.
- [15] S. Adsule, V. Barve, D. Chen, F. Ahmed, Q.P. Dou, S.B. Padhye, F.H. Sarkar, *J. Med. Chem.* 49 (2006) 7242–7246.
- [16] A.I. Vogel, *A Text Book of Quantitative Inorganic Analysis*, third ed., Longman Green and Co. Ltd., London, 1961.
- [17] A.K. Sen, S.K. Gupta, *J. Ind. Chem. Soc.* 39 (1962) 628–634.
- [18] M.S. Shahabuddin, M. Gopal, Sathees C. Raghavan, *J. Cancer Mol.* 3 (2007) 139–146.
- [19] J.A. Glasel, *Biotechniques* 18 (1995) 62–63.
- [20] N. Li, Y. Ma, C. Yang, L. Guo, X. Yang, *Biophys. Chem.* 116 (2005) 199–205.
- [21] S. Satyanarayana, J.C. Dabrowiak, J.B. Chaires, *Biochemistry* 31 (1992) 9319–9324.
- [22] S. Arounaguiri, B.G. Maiya, *Inorg. Chem.* 35 (1996) 4267–4270.
- [23] A. Arslantas, A.K. Devrim, H. Necefoglu, *Int. J. Mol. Sci.* 8 (2007) 564–571.
- [24] W.J. Geary, *Coord. Chem. Rev.* 7 (1971) 81–122.
- [25] V.K. Reddy, *Indian J. Chem.* 41A (2002) 2046–2053.
- [26] S. Budagumpi, M.P. Sathisha, N.V. Kulkarni, G.S. Kurdekar, V.K. Revankar, *J. Incl. Phenom. Macrocycl. Chem.* 66 (2010) 327–333.
- [27] A.B.P. Lever, *Inorganic Electronic Spectroscopy*, Elsevier Publishing Company, New York, 1968.
- [28] J.C. Bailar, H.J. Emeleus, R. Nyholm, A.F.T. Dickenson, *Comprehensive Inorganic Chemistry*, vol. 3, Pergamon Press, 1975.
- [29] A.E. Martwell, M. Calvin, *Chemistry of the Metal Chelate Compounds*, Prentice Hall, New York, 1952. p. 214; R.L. Dutta, A. Syamal, *Elements of Magnetochemistry*, second ed., EW Press, 1993.
- [30] M. Munakata, L.P. Wu, M. Yamamoto, T. Kuroda-Sowa, M. Maekawa, S. Kawata, S. Kitagawa, *J. Chem. Soc. Dalton Trans.* (1995) 4099–4106.
- [31] C.L. Bailey, R.D. Bereman, D.P. Rillema, *Inorg. Chem.* 25 (1986) 3149–3153.
- [32] P.J. Lukes, A.C. McCregor, T. Clifford, J.A. Crayston, *Inorg. Chem.* 31 (1992) 4697–4699.
- [33] A. Shah, R. Qureshi, A.M. Khan, R.A. Khera, F.L. Ansari, *J. Braz. Chem. Soc.* 21 (2010) 447–451.
- [34] V.A. Bloomfield, D.M. Crothers, I. Tinoco, *Physical Chemistry of Nucleic Acids*, Harper and Row, New York, 1974. pp. 432–434; A.M. Pyle, J.P. Rehmann, R. Meshoyrer, C.V. Kumar, N.J. Turro, J.K. Barton, *J. Am. Chem. Soc.* 11 (1989) 3051–3058.
- [35] V. Rajendiran, R. Karthik, M. Palaniandavar, H. Stoeckli-Evans, V.S. Periasamy, M.A. Akbarsha, S.S. Bangalore, H. Krishnamurthy, *Inorg. Chem.* 46 (2007) 8208–8221.
- [36] A. Arslantas, A.K. Devrim, N. Kaya, N. Necefoglu, *Int. J. Mol. Sci.* 7 (2006) 111–118.